2.671 Measurement and Instrumentation
Wednesday PM
Prof. Sili Deng
05/07/2024

MODELING THE FORCE RESPONSE OF A LINEAR MOTOR SYSTEM FOR VARYING POSITION AND CURRENT

Andy Dequin
MIT Department of Mechanical Engineering
Cambridge, MA, USA

ABSTRACT

Linear brushless motors are characterized by their ability for precision motion control and energy efficiency. They are used across a variety of industrial applications, ranging from plant automation to superconducting maglev trains. The system in question for this study is a lightweight, low complexity, and low-cost magnetic linear brushless motor suitable for rapid prototyping or for hobbyist applications. The open-loop control of the position is not straightforward due to significant end effects, friction, nonlinearities in the magnetic interactions, and the lack of mechanical commutation—all aspects of the motor that are directly related to the force response that drives the system. It was found that the force can be reasonably modeled as the linear combination of the position and current independently over 70% of the range of motion. Using this model facilitates the design of a compensating controller by allowing the system to be analyzed as an LTI system.

Keywords: brushless DC linear motor, linear motor dynamics, linear motor design, linear motor controls

INTRODUCTION

This research draws inspiration the from magically actuated floating blocks portrayed in Castle in the Sky by Studio Ghibli [7]. The portrayed system of actuation exhibits an opportunity for using a linear brushless motor as a modular actuation system. More specifically, the characterization of the force response of the blocks could make more accessible the design of a lightweight, low complexity, and low-cost magnetic linear actuation for a rapid prototyping step in a larger project or for hobbyist applications. Linear brushless motors are characterized by their ability for precision motion control and energy efficiency. They are used in robotic systems requiring rapid movements and high precision, such as manufacturing and medical devices, as well as larger-scale high-speed systems like maglev trains and mass drivers. While the working principle is well modeled and understood, to account for variations between specialized applications, the dynamics are determined experimentally in this research.

The linear motor that was studied has significant friction and gaps between the magnetic fields that other studies may have ignored [3]. Due to these significant end effects, the motor currently exhibits undesirable thrust ripples when driven by a square wave input across many frequencies. By modeling the force as a function of current and spacing, this study lays the foundation for the design of a controller that would compensate for these undesired oscillations.

To better understand the force response, the relationship between the force and the input variables, position and current, was determined. To record these measurements, the experiment uses a force sensor, position markings, and a direct current probe. While the original model has two coils offset by half a period, it can be reconstructed by superposition of the single coil force response. Following this idea, the simplified tested model consists of two cube-shaped 3D-printed nylon frames placed side-by-side. One contains a row of four evenly spaced permanent magnets imbedded into one of the side faces, and the other contains two side-by-side electromagnets facing the frame's side panels.

BACKGROUND AND THEORY

To model the data of the force response, it is helpful to predict its relationship with the system's geometry, material characteristics, and electric current. To motivate the significance of this study, relevant terminology and variations with electric motors are introduced, the force response is constructed from the motor components and fundamental equations, the analyzed response is contextualized within the dynamic model of the motor system, and supporting research is discussed.

MOTOR TYPES AND TERMINOLOGY

The focus of the study will be on linear brushless DC motors. While there is plenty of variety in electric motors, DC and AC, brushed, synchronous, etc., they all typically generate force due to the interaction between magnetic fields. In brushless motors, permanent magnets on the moving part (i.e., rotor, slider, or mover) are affected by the magnetic fields generated from current-conducting coils of wire in the static part (i.e., the stator). Conventional

rotating brushed motors operate on a similar principle, except with the current flowing between the rotating shaft (the rotor) and the fixed outer frame dynamically. Fixed brushes, located on the stator, give current to the coil they physically touch and, in doing so, close a circuit. Due to the physical contact and arcing in a brushed motor, the parts wear down and must be maintained. One of the main advantages of the brushless motor is the lack of brushes, which reduces inefficiencies and maintenance needs due to physical contact.

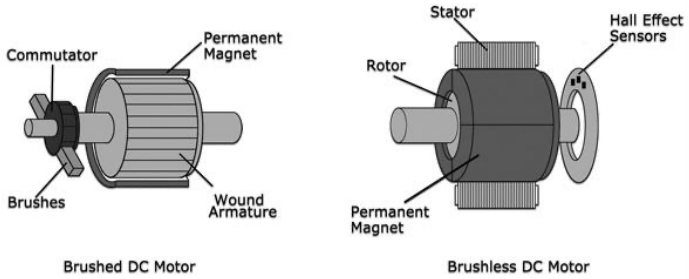

Figure 1: Diagram comparing brushed and brushless DC motor mechanisms [1]

A linear brushless motor is comprised of moving permanent magnets atop a bed of electromagnets. Although linear motion can also be created from optimized rotating motors with the help of gears and belts, linear motors have the advantage of requiring fewer moving parts and maintenance.

LINEAR MOTOR FORCE COMPONENTS

For the system in question, there are three main contributions to the force response: the attraction of the iron core to the permanent magnets, the current-induced magnetic field in the coil, and the friction forces between frame surfaces.

The relationship with the current can be estimated using fundamental equations. The current-induced magnetic field in the iron core multiplies according to Ampere's law for solenoids Eq. (1), which is directly related to the force through Lorentz force law Eq. (2) [5] and Coulomb's law for magnetism Eq. (3) [6].

$$B = \frac{\mu N i}{L} \quad (1)$$

$$\vec{F} = \int \vec{B} \times \vec{\imath} dl \quad (2)$$

$$F = \frac{\mu_0 m_1 m_2}{4\pi r^2} \quad (3)$$

Where μ is the magnetic permeability of the material in the core of a solenoid, i is the electrical current flowing through the coil, F is the resulting force, B is the magnetic field, m_1 and m_2 are the magnetic moments of each dipole, and r is the distance between the centers of the dipoles.

For this study, since these experimental conditions are far from the idealized environment where these formulas hold, we will be determining empirically the variations in attraction using the current parameter i and distance r to modulate the force response. What these equations do show is that the output force will likely be proportional to the input current and distance, as these parameters vary when operating the motor.

Note that the iron core significantly amplifies the force produced and can be cheaper and easier to implement than air cores [5]. It also produces, however, an additional attraction force component that complicates modeling the force response. Fig. 2 describes the components of the test model and identifies the interaction forces acting on the moving frame. The positive and negative bias labels indicate the direction of current flowing through the electromagnet.

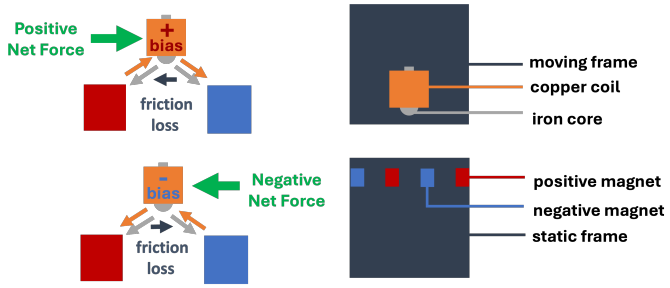

Figure 2: Force interactions in the test model between the permanent magnets, the electromagnets, and the iron core.

It is observed that in between the permanent magnets, the current-induced force dominates, whereas closer to one of the magnets, the iron core force is significant, and significantly contributes to the normal force and resulting friction. When roughly aligned with a magnet, the actuator is trapped as there is no transversal component to the current-induced force, and the friction due to iron core attraction is maximized. Through this observation, it is clear that the position plays a significant role in the motor's response.

MOTOR CONTROL ARCHITECTURE

Within the linear brushless motor, there are several subsystems that describe the path from the desired input to the output. While most components are readily derived or approximated, the complex dynamic magnetic interactions that produce the force may be strongly nonlinear. A linear time invariant (LTI) approximation of this system would

allow the construction of the transfer function that maps the current input to the position output for the linear regime. Using symmetry and accounting for disturbances, we could then simulate the resulting motion of the motor based current inputs for the whole range. Using this transfer function of an LTI system, the process of matching controller and response specifications is simplified. Fig. 3 shows how the force response fits into the broader dynamics of the whole linear brushless motor model, including the coil dynamics and feedback paths that the actual system would experience.

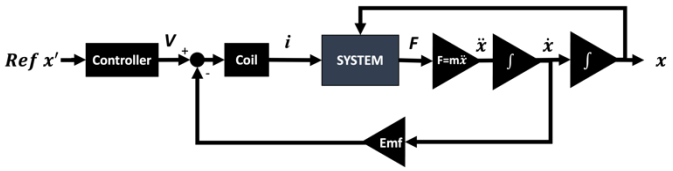

Figure 3: Block diagram of the linear motor for position tracking. The block labeled SYSTEM represents the unknown dynamics that were modeled in this study. x' is the reference position, V is the control voltage, i is the current, F is the force response, and x, $\dot{x}$, and $\ddot{x}$, are the position, velocity, and acceleration, respectively.

In the context of other electric motors, mechanically commutated motors often have a linear characteristic parameter, the motor constant K_T, where the torque and speed are linearly related and there is a direct relationship with the current and voltage. Electrically commutated motors have a more indirect response as a function of the phase alignment between the magnet spacing and the current input frequency and cannot be assumed to behave linearly. Therefore, instead of tracking the motion data, we will only be measuring the static force generated at a constant load in order to isolate the force response from feedback paths and to model the direct relationship with current and position.

EXPERIMENTAL DESIGN

Due to the symmetry of the system, there is an unstable equilibrium when the electromagnet is set to 0 mm (see Fig. 4), as well as a stable equilibrium when aligned with one of the magnets (>8 mm). Since the system is cyclical, analyzing the force response around both equilibriums would allow for modeling of the whole range through a piecewise representation. In this section, the system parameters are provided, the signal generation and sensing apparatus are introduced, their uses are described, and the calibration and data acquisition procedures are outlined.

MOTOR SYSTEM PARAMETERS

The system parameters in Table 1 are values that describe the system from the block diagram in Fig 3. They are used to determine the broader input-output position relationship of the overall system and to validate the experiment results.

Table 1: Measured system parameters

Parameter	Value
Coil resistance (iron core)	$26.468 \pm 0.004\ \Omega$
Coil inductance (iron core)	1×10^{-4} H
Average normal static friction force	$0.166 \pm 0.029N$
Frame-table static friction coefficient	$0.17 \pm 0.03\ \frac{N}{N}$
Frame to frame static friction coefficient	$0.33 \pm 0.02\ \frac{N}{N}$

The coil resistance was determined using an HP 34401A Multimeter 4-wire resistance measurement at room temperature. The inductance was found by recording the current response to a 24 Vpp ramp input using a Vernier direct current probe and identifying the time constant. The static friction values were determined by using a Vernier dual-range force sensor set to 10 N, pushing the static frame until it moved, and identifying the peak value. This experiment was repeated four times, and the value was averaged.

3.2 CURRENT, POSITION, AND FORCE APPARATUS

Determining the force response as a function of current and position requires a generated electric current input, sensors to track the input current and position, as well as a sensor for the output force. The apparatus responsible for sensing and producing the input signal is presented in Table 2.

Table 2: Specifications of the instruments used in the experiment

Quantity	Instrument	Use	Units	Range	Resolution
Distance	Pen Markings	Measure	Millimeter	±10 mm	1 mm
Current	Vernier Direct Current Probe	Measure	Ampere	±10 A	4.9 mA
Force	Vernier Dual-range Force Sensor	Measure	Newton	±10 N	0.01 N
Voltage	Function Generator FG 33220A	Input	Volts	±5 V	N/a
Voltage	Vernier Power Amplifier (x20)	Input	Volts	±12 V Input ±12 V Output	N/a

A Vernier Dual-range Force Sensor was used with the flat attachment to measure force in one direction, and a Vernier Direct Current Probe was used to measure the current flowing through the electromagnet. Pen markings were created using a ruler directly on the frame to which the magnets are fixed. They were used to determine the spacing between the electromagnets and permanent magnets. The experiment setup is described in the next section.

FORCE SENSING SETUP

To collect force data, an input current signal was passed through the electromagnet, which produced a system force response (presented in Fig. 2) that the force sensor recorded. The system is comprised of a single electromagnet with an iron bolt core facing a set of permanent magnets with opposing polarities. The magnets are affixed to their respective motor frames, and the frame containing the permanent magnets was clamped to the table. While the force sensor only captures force in one direction, using the symmetry of the system response around position 0 mm (equidistant to the magnets), partial data was recorded over the entire range, then inverted, negated, and added onto the positive data to construct the response over the complete current range (see Fig. 5).

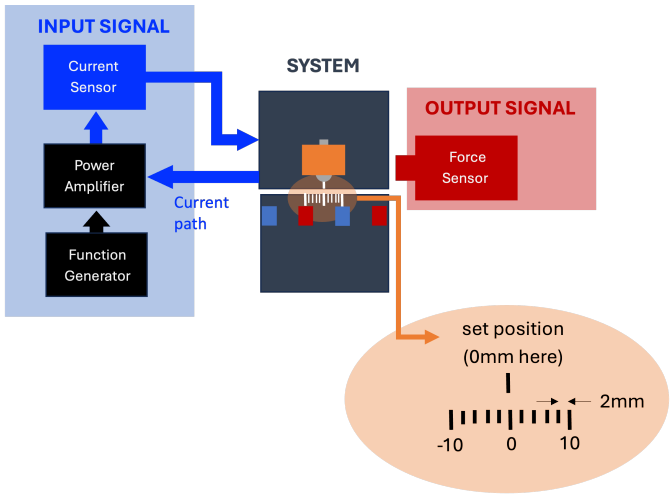

Figure 4: Layout of the instruments used in the experimental setup. The input signal generation and sensing are described (left), the SYSTEM and position tracking are specified (center), and the resulting force output is measured (right).

To produce the input current, a function generator was set to produce a ramp input of 600 mV peak-to-peak with a period of 2 s. The signal was amplified by the power amp to produce a ramp input of 12 V peak-to-peak and a 2 s period. The input current was then measured through the direct current probe, wired in series between the power amplifier and the electromagnet.

The position of the coil at which each test occurs was recorded by aligning the set position with the 2 mm markings. Increments of 1 mm were achieved by placing the set position in between two markings. The force response of the system was measured with the dual-range force sensor, which was held in place by hand during each experiment.

3.4 EXPERIMENT PROCEDURE AND CALIBRATION

The experimental procedure is as follows. To set up a trial, the sensors are first calibrated in Logger Pro (to an error below instrument resolution), and the coil is then moved to the next position. To begin the trial, the function generator output is triggered. For data collection, the force sensor is aligned to the motion path (near the frame edge), and a Logger Pro trigger is set to -0.4 A, the beginning of the input current ramp. After two seconds, the force is inspected to make sure that it eventually reaches 0 N, if appropriate. The file is then saved and the .csv file is

exported for post-processing in Matlab. The experiment is repeated three times for each 1 mm increment.

The experiment was repeated three times per position between positions -7 mm to 7 mm with 1 mm increments for a total of 45 trials. The distances of 8 mm to 10 mm from the 0 mm positions were discarded as the force response was insufficient to move the motor; any data in this case would be a result of static friction holding the force sensor against the motor frame. When tests are repeated too quickly, the coil may heat up and increase its resistance, reducing the range of current values for that trial. This is accounted for by setting the data collection trigger at -0.4 A so that the trial only begins if the -0.4 A to -0.4 A range is available.

RESULTS AND DISCUSSION

To model the force response of the linear brushless DC motor, data was collected at varying current and position values in the 2cm range between the magnets. With the data collected, it was possible to determine if a linear approximation is suitable to model the linear motor's force response around the unstable and stable equilibriums. Finding a linear approximation allows for the construction of the system transfer function and facilitates the design of a controller that can correct for the current jittery motion. In this section, the processed data is presented, a linear model is applied, the significance and limitations of the data are considered, and an outline for further research is proposed.

COMBINING FORCE DATA

As explained in Section 3.3, single-direction force data was collected over the entire position range. As the current reaches a threshold value, the force applied to the motor changes direction, and the recorded force value stays at 0 N. To obtain force data over the complete current range, the force values with initial positions of less than 0 mm were inverted and negated and combined with the position range between 0 mm and 7 mm. Due to placing the origin at the axis of symmetry of the magnet array, negating the applied current has the same effect on force output as negating the starting position. The inversion and negation are represented in Fig. 5, where paired values are colored the same.

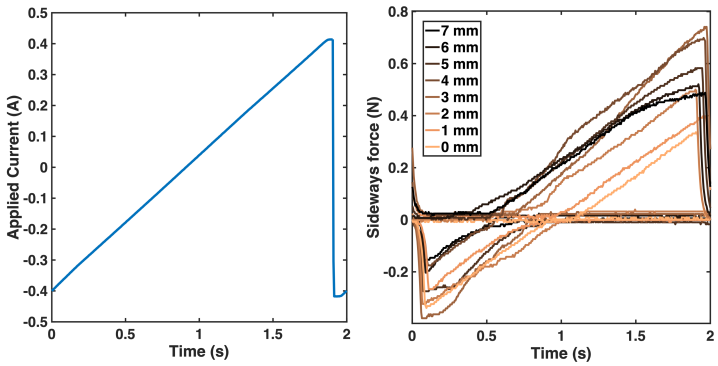

Figure 5: The input ramp current (left) and the output force response of the motor to the ramp current (right).

To combine the data, the largest absolute value between the paired force values was selected for each current and position input. After collecting the data over the range of 0 mm to 7 mm, the range can be extended by inverting the order and negating the value.

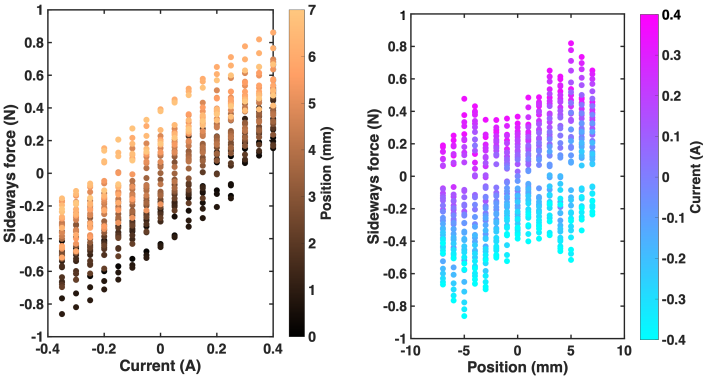

Figure 6: Combined force data as a function of current for each position rotated around symmetry point 0 mm for model fitting.

The force data in Fig. 6 was retrieved from the initial ramp response by selecting 16 discrete current values between -0.35A and 0.4A for clarity. The lower bound of -0.35A was chosen instead of -0.4A to account for a slight delay in the force response. This delay is visible in the combined data, where the slight offset leads to a slight mismatch between the current and the force data and results in a discontinuous transition between the positive and negative forces. An improved setup would measure both directions simultaneously for more homogenous values.

FITTING FORCE DATA

To model the two variable data linearly, ideally, we would like to have a reliable fit using a first-order polynomial model with no cross terms. From Section 2.2 of the background, we can expect to see that there is a contribution from the position, the current, as well as friction, which also acts like an absolute value filter with a position-dependent threshold. Combining the position-dependent contributions and assuming that the sideways force overcomes friction, the model can be simplified to $p_{01}x + p_{10}i$, where x is the position and i is the current. The planar fit model is shown in Fig. 7. A nonlinear model can also be constructed from the sum of two sine waves, with a frequency ratio of 1:2 and no phase shift.

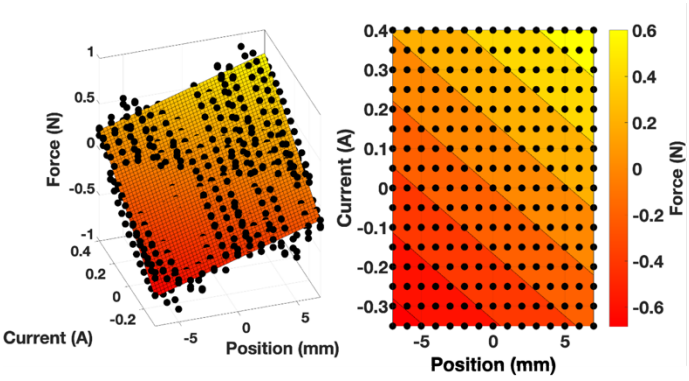

Figure 7: First-order polynomial planar fit of the motor force response.

In Fig. 7, position 0 mm represents the unstable equilibrium position between the magnets at -10 mm and 10 mm. The fit model has the form $F(x, i) = p_{01}x + p_{10}i$ where F is the force, x is position, and i is the current. Parameters $p_{01} = 37.8 \pm 1.9 \frac{N}{m}$ and $p_{10} = 1.1978 \pm 0.036 \frac{N}{A}$. The R^2 term is 0.8915 and the RMSE is 0.1125 N for this fit. This indicates a positive correlation between increasing distance away from the equilibrium point and increasing current applied through the electromagnet, with an increasing resulting force.

As indicated by the RMSE value of 0.1125 N, which is almost 20% of the maximum magnitude, the model does not predict the values very precisely, even within the linear range. Additionally, patterns in the residuals clearly indicate that there are some unmodeled non-linear dynamics present in the data. For the purposes of this study, however, the linear model shows an adequate correlation with the data that is sufficient for moving forward.

Note that while the values near the magnet are not significant and were dropped, there is still some non-linear behavior affecting the residuals in the transition region where the normal friction starts to significantly reduce the force output. The limit behavior is not very responsive, and an adequate linear model seems to describe 70% of the motor's range of motion. In the actual two-coil motor system where a secondary coil is out of phase, the coil in the non-linear range can be set to reduce the friction due to iron core attraction or simply turned off. To simulate the motion of the motor over the full range, the static friction threshold values near the magnet remain to be determined.

With this model, the unknown SYSTEM block introduced in Fig. 3 can be specified to produce the updated diagram, Fig. 8. In the updated system diagram, the model is used to separate the terms, approximating them as linearly independent. The peripheral blocks can also be filled in using the system parameter values from Section 3.1.

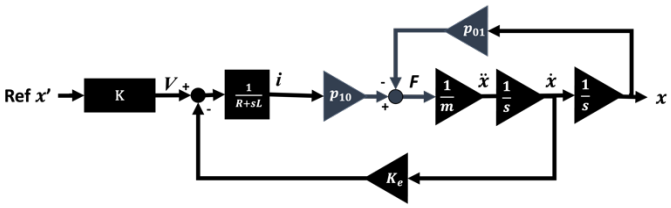

Figure 8: Updated block diagram using the force response model. Simplifying the inductor block to $\frac{1}{R}$ at low frequencies and ignoring emf, the transfer function was computed to be $G(s) = \frac{p_{10}}{R(ms^2 - p_{01})}$

To extend this study, further research could involve modeling the friction force in the 3 mm region near the permanent magnets, simulating the two-coil system by combining the force response from this study and the resulting friction model as a piecewise response. The simulated dynamics could then be compared to the motion of the actual system to validate the model. Once validated, the model can be used to derive an initial controller design for smooth motion.

CONCLUSIONS

While a force related to the squared inverse of the distance to the magnets or more complex nonlinearities might have been expected, a linear model was found to be a good approximation for 70% of the range of motion. With the model approximating the force response as the sum of current and position with linear scaling coefficients, it is now possible to determine a transfer function and simulate the system response. The transfer function provides a starting point for modeling similar lightweight,

low complexity, and low-cost magnetic linear brushless motor suitable such as for rapid prototyping or hobbyist applications. Further research would involve designing a suitable controller for the linear brushless motor system and validating the simulation data with motion tracking.

ACKNOWLEDGMENTS

The author would like to gratefully acknowledge helpful discussions with Prof. Deng, Dr. Hughey, Kevin DiGenova, and Rachel Molko.

REFERENCES

[1] Y. Zhu and Y.-H. Cho, "Thrust ripples suppression of permanent magnet linear synchronous motor," *IEEE Transactions on Magnetics*, vol. 43, no. 6, pp. 2537–2539, Jun. 2007. doi:10.1109/tmag.2007.893308

[2] Barrett, J., 2009. Linear Motors Basics. [Online] Available at: http://www. parkermotion.com/ whitepages/linearmotorarticle.pdf

[3] L. Ruozhu, Y. Qingdong, and T. Liang, "Thrust ripples test and analysis of permanent magnet linear synchronous motor," *2011 Third International Conference on Measuring Technology and Mechatronics Automation*, Jan. 2011. doi:10.1109/icmtma.2011.825

[4] X. Lu, Y. Li, and Z. Chen, "Temperature field analysis and cooling structure design of ironless permanent magnet synchronous linear motor," *Recent Advances in Electrical & Electronic Engineering (Formerly Recent Patents on Electrical & Electronic Engineering)*, vol. 15, no. 1, pp. 24–30, Feb. 2022. doi:10.2174/2352096514666211123090446

[5] Adel. Ismael and F. J. Anayi, "Modelling of a prototype brushless permanent magnet DC linear stepping motor employing a flat-armature winding configuration," *2016 Third International Conference on Electrical, Electronics, Computer Engineering and their Applications (EECEA)*, Apr. 2016. doi:10.1109/eecea.2016.7470771

[6] E. Technology, "Coulomb's laws of magnetic force - formula & solved example," ELECTRICAL TECHNOLOGY, https://www.electricaltechnology.org/2020/12/coulombs-laws-of-magnetic-force.html (accessed Apr. 18, 2024).

[7] "Final project," HTMAA Final Project, https://fab.cba.mit.edu/classes/863.23/CBA/people/Andy/FinalProject.html (accessed Apr. 24, 2024).